ARTICLE - Hematopoiesis

Protein phosphatase 2A orchestrates hematopoietic fate determination via modulation of lactate metabolism

Can Liu,[1*] Yao Meng,[1,2*] Heng Chen,[3*] Siqi Bi,[1*] Ye Tian,[1] Zhihua Yin,[4] Guanhua Li,[5] Wutao Chen,[6] Li Wu,[7] You Wang,[6] Nan Shen,[1,8-11] and Haibo Zhou[1]

[1]Shanghai Institute of Rheumatology, Renji Hospital, School of Medicine, Shanghai Jiao Tong University (SJTUSM), Shanghai, China; [2]Department of Nephrology, Zhongshan Hospital, Fudan University, Shanghai, China; [3]The Affiliated Wuxi People's Hospital of Nanjing Medical University, Wuxi People's Hospital, Wuxi Medical Center, Nanjing Medical University, Wuxi, China; [4]Shenzhen Futian Hospital for Rheumatic Diseases, Shenzhen, China; [5]Department of Nephrology, The First Affiliated Hospital of Zhengzhou University, Zhengzhou, China; [6]Department of Obstetrics and Gynecology, Renji Hospital, School of Medicine, Shanghai Jiao Tong University (SJTUSM), Shanghai, China; [7]Tsinghua-Peking Joint Center for Life Sciences, Tsinghua University School of Medicine, Beijing, China; [8]China Australia Center for Personalized Immunology, Renji Hospital, School of Medicine, Shanghai Jiao Tong University (SJTUSM), Shanghai, China; [9]State Key Laboratory of Oncogenes and Related Genes, Shanghai Cancer Institute, Renji Hospital, Shanghai Jiao Tong University School of Medicine (SJTUSM), Shanghai, China; [10]Center for Autoimmune Genomics and Etiology (CAGE), Cincinnati Childrens Hospital Medical Center, Cincinnati, OH, USA and [11]Department of Pediatrics, University of Cincinnati College of Medicine, Cincinnati, OH, USA

**CL, YM, HC, and SB contributed equally as first authors.*

Correspondence: H. Zhou
hbzhou1984@163.com

N. Shen
nanshensibs@gmail.com

Y. Wang
wanghh0163@163.com

Received: August 11, 2025.
Accepted: November 6, 2025.
Early view: November 13, 2025.

https://doi.org/10.3324/haematol.2025.288868

Supplementary Methods

Cell preparation and flow cytometry analysis

Single cells from murine spleen and BM were prepared as previously described. Briefly, splenocytes were enzymatically digested with 1 mg/mL collagenase IV (C5138, Sigma-Aldrich) and 10 μg/mL DNase I (10104159001, Roche) at 37°C for 30 min. Red blood cells were then lysed using red cell lysis buffer (00-4333-57, ThermoFisher Scientific). Single-cell suspensions were prepared by passing through a 70-μm cell strainer. To block non-specific binding, cells were incubated with anti-mouse CD16/32 antibody (101302, BioLegend, 1:200) at 4°C for 15 min. Cells were subsequently stained with fluorochrome-conjugated antibodies (1:200) for 30 min at 4°C in the dark, followed by washing with PBS. For live-cell discrimination, cells were stained with BD Horizon™ Fixable Viability Stain 575V (565694, BD Biosciences, 1:1000) at room temperature for 10 min. After washing with staining buffer (420210, BioLegend), cells were analyzed using a BD LSRFortessa flow cytometer, and data were processed with FlowJo v10 software. A detailed list of antibodies used in this study is provided in Supplementary Table 1.

Lin^- cells were obtained by depleting lineage cells using a combination of rat-anti-mouse antibody cocktails (CD2, CD3, CD8, CD11b, Gr-1, Ter-119, CD19, B220) and anti-rat secondary antibody conjugated with magnetic beads (Biomag).

ROS analysis via flow cytometry

Total ROS levels in BM LSK cells were detected using CellROX™ Green Reagent (C10492, ThermoFisher Scientific). Cytosolic and mitochondrial ROS was detected with DCFH-DA (cytosolic ROS-preferential probe, Catalog No.: C6827, ThermoFisher Scientific) and MitoSOX™ Red Reagent (mitochondrial ROS-specific probe, Catalog No.: M36008, ThermoFisher Scientific), respectively. Isolated BM LSK cells (2×10^5) were resuspended in 200 μL serum-free RPMI 1640 medium and incubated with 500 nM CellROX™ Green Reagent, 500 nM MitoSOX™ Red Reagent or 1 μM DCFH-DA at 37°C for 30 min in the dark. After two washes with PBS, cells were immediately analyzed by flow cytometry (BD LSRFortessa). The mean fluorescence intensity (MFI) of CellROX™ Green, MitoSOX™ Red and DCFH-DA was recorded to quantify total, mitochondrial, and cytosolic ROS levels, respectively.

Measurement of NAD+/NADH ratio

The NAD+/NADH ratio in BM LSK cells was determined using the NAD+/NADH Assay Kit (ab176723, Abcam) following the manufacturer's instructions. Briefly, 1×10^6 BM LSK cells were collected and lysed in 25 μL of the provided lysis buffer for 10 min. After centrifugation at 400 × g for 5 min, the supernatant was transferred to a 96-well plate. For each sample well, 25 μL of NAD or NADH extraction solution was added, followed by 75 μL of reaction mixture. The plate was incubated at 37°C for 1 h, and absorbance was measured at a wavelength of 576 ± 5 nm using a colorimetric microplate reader. The NAD+/NADH ratio was calculated based on the

standard curve generated with the provided standard solutions. All experiments were performed in triplicate.

Cell culture and transfection

LSK or Lin^- cells were cultured in Roswell Park Memorial Institute (RPMI) 1640 (Gibco) containing L-glutamine, supplemented with 10% Fetal Bovine Serum (FBS, Gibco), 1% Penicillin-Streptomycin (Gibco) and 0.1% 2-Mercaptoethanol (Gibco). Lin^- cells were treated with or without 10mM sodium oxamate (Selleck). 293FT cell line was cultured in Dulbecco's Modified Eagle Medium (DMEM, Gibco) containing L-glutamine supplemented with 10% FBS (Gibco) and 1% Penicillin-Streptomycin (Gibco).

For lentiviral transfection, mouse Lin^- cells were pre-stimulated with 100ng/mL SCF, 100ng/mL Flt3L and 100ng/mL TPO for 24 hours. Then, cells were subjected to centrifugal transfection at 37℃, 1000g for 1 hour. After that, cells were washed and prepared for subsequent studies.

Plasmid construction

The coding regions of murine HDAC1 (NM_008228) and HDAC2 (NM_008229) were synthesized and cloned into the multiple cloning sites of the EF1α-MCS-Flag-PGK-EGFP lentiviral plasmid (Tsingke Biotech, China). The mutant forms of HDAC1 and HDAC2 were constructed by using the KOD -Plus-

Mutagenesis Kit (TOYOBO, Japan).

RNA sequencing

Total RNA was extracted by Trizol reagent (Invitrogen). RNA libraries were prepared using the VAHTS mRNA-seq v2 Library Prep Kit for Illumina® (Vazyme, Nanjing, China) and sequenced on the Novaseq 6000 system (Illumina, San Diego, CA, USA). Genes with *p* value less than 0.05, as determined by DESeq2 analysis, and log2 fold change greater than 0.5 were selected for further analysis. Kyoto Encyclopedia of Genes and Genomes (KEGG), Gene Ontology (GO) and Gene Set Enrichment Analysis (GSEA) were used to determine the enriched pathway of selected genes.

Immunoblots and co-immunoprecipitation

3×10^6 primary cells were lysed using RIPA protein exaction buffer (Thermo Fisher Scientific). Subsequently, the cell lysates (10μg/lane) were separated by 10% SDS-PAGE and transferred onto an Immobilon-P polyvinylidene difluoride membrane (Millipore, Billerica, MA). Then, the membrane was blocked with SuperBlock TBS blocking buffer (Thermo Fisher Scientific) and incubated with indicated antibodies listed in the Supplementary Table 1. Gels analysis was performed using Image J software.

Lysates were prepared from 1×10^7 cells transfected with HDAC1-Flag or HDAC2-Flag, followed by immunoprecipitation of HDAC protein using an anti-Flag

antibody (Cell Signaling Technology) and the Pierce™Classic Magnetic IP/Co-IP Kit (Thermo Fisher Scientific). The precipitated protein was detected by immunoblotting.

CUT&Tag and CUT&RUN

A total of 1×10^5 LSK cells were prepared by using the Hyperactive Universal CUT&Tag Assay Kit for Illumina (Vazyme, China) according to the protocol. The trimmomatic software was employed to remove adapters and low quality reads[24]. Before read mapping, clean reads were obtained from the raw reads by removing the adaptor sequences. The clean reads were then aligned to the GRCm38/mm10 genome sequences using the bwa program. The bam files were subjected to macs2 software for peak calling with cut off q value < 0.05. Reads distributions across peaks or genes were analyzed with the deeptools. The HOMER's findMotifsGenome.pl tool was used for motif analysis and peaks were annotated by ChIPseeker. For CUT&RUN, LSK cells were subjected to the Hyperactive pG-MNase CUT&RUN Assay Kit for Illumina (Vazyme, China). H3K27ac occupied sites with more than 1 fold change and *p* values less than 0.05 were selected for further analysis.

Metabolomics study

The metabolites in LSK cells were detected using the Q300 Kit provided by Metabo-Profile (Shanghai, China). Cell samples previously stored at −80℃ were subjected to a quantitative UPLC-MS/MS platform (ACQUITY UPLC-Xevo TQ-S, Waters Corp., MA, USA). The raw data files generated by UPLC-MS/MS were

processed using the TMBQ software (v1.0, Metabo-Profile, Shanghai, China) to perform peak integration, calibration, and quantitation for each metabolite. The XploreMET platform (version 4.0; Metabo-Profile, Shanghai, China) was used for statistical analysis, including principal component analysis (PCA), orthogonal partial least squares discriminant analysis (OPLS-DA), univariate analysis and pathway analysis.

Lactylation modified proteomics

The sample was grinded into cell powder with liquid nitrogen and lysed, followed by sonication for three minutes on ice using a high intensity ultrasonic processor (Scientz). Then, the supernatant was collected and protein was precipitated with the final concentration of 20% (m/v) TCA. The protein digestion was conducted overnight with the addition of trypsin at a trypsin-to-protein mass ratio of 1:50, followed by the peptides collection using Strata X SPE column. To enrich modified peptides, tryptic peptides dissolved in NETN buffer (100 mM NaCl, 1 mM EDTA, 50 mM Tris-HCl, 0.5% NP-40, pH 8.0) were incubated overnight at 4℃ with pre-washed agarose beads conjugated with anti-L-lactyllysine antibody (PTM Bio, PTM-1404). The bound peptides were eluted from the beads with 0.1% trifluoroacetic acid. For LC-MS/MS analysis, the obtained peptides were desalted with C18 ZipTips (Millipore) and dissolved in solvent A before being directly loaded onto a home-made reversed-phase analytical column (25-cm length, 100 μm i.d.). The mobile phase consisted of solvent A (0.1% formic acid, 2% acetonitrile/in water) and solvent B

(0.1% formic acid in acetonitrile). Peptides were separated with following gradient: 0-40 min, 6%-24% B; 40-52 min, 24%-35% B; 52-56 min, 35%-80% B; 56-60 min, 80% B, and all at a constant flow rate of 450nl/min on a NanoElute UHPLC system (Bruker Daltonics). Finally, peptides were subjected to capillary source followed by the timsTOF Pro mass spectrometry.

The MS/MS data were processed using the Maxquant search engine (v.1.6.15.0). Tandem mass spectra were searched against Mus_musculus_10090_SP_20220107.fasta (17097 entries) concatenated with reverse decoy database. Carbamidomethyl on Cys was specified as a fixed modification, and oxidation of methionine, N-terminal acetylation of protein, and lactylation of lysine were specified as variable modifications. FDR was adjusted to less than 1%.

Transcriptome Principal Component Analysis (PCA)

PCA was performed on the entire transcriptome dataset. Gene filtering: All expressed genes were filtered based on the average read count, with a threshold of average read count > 10 to retain high-confidence expressed genes for subsequent analysis. Data normalization: Variance-stabilized normalization was applied to the filtered gene count data to reduce technical variation and ensure data comparability across samples. PCA execution: The PCA was conducted using the prcomp function integrated in the stats package of R software. This function was used to compute the principal components (PCs) of the normalized transcriptome data. Visualization: The first two

principal components (PC1 and PC2) derived from the PCA were selected for visualization. Scatter plots were generated to map each sample onto the coordinate system defined by PC1 and PC2, with samples from the WT and KO groups labeled separately to illustrate transcriptomic clustering patterns.

Unbiased Identification of Genes Driving Condition-Specific Transcriptomic Differences

Differential expression analysis was re-conducted to screen for genes with significant expression differences between WT and KO groups, using the DESeq2 package in R software. Strict filtering thresholds were set to ensure the reliability of differentially expressed genes (DEGs): Adjusted p-value (padj) < 0.01 (to control for false discovery rate); Absolute log2 fold change (|log2FC|) > 1 (to ensure a minimum magnitude of expression change between groups).

To further prioritize genes that drive the transcriptomic separation of WT and KO groups, a "contribution score" was calculated for each DEG. The score was defined as the product of two metrics: ① Absolute log2 fold change (|log2FC|) of the DEG: Reflects the magnitude of expression difference between WT and KO groups; ② Loading value of the DEG on the first principal component (PC1): Reflects the strength of correlation between the DEG' s expression and the primary source of transcriptomic variance (i.e., the "condition" of WT vs. KO) identified in PCA. Genes were then ranked in descending order based on their calculated contribution scores.

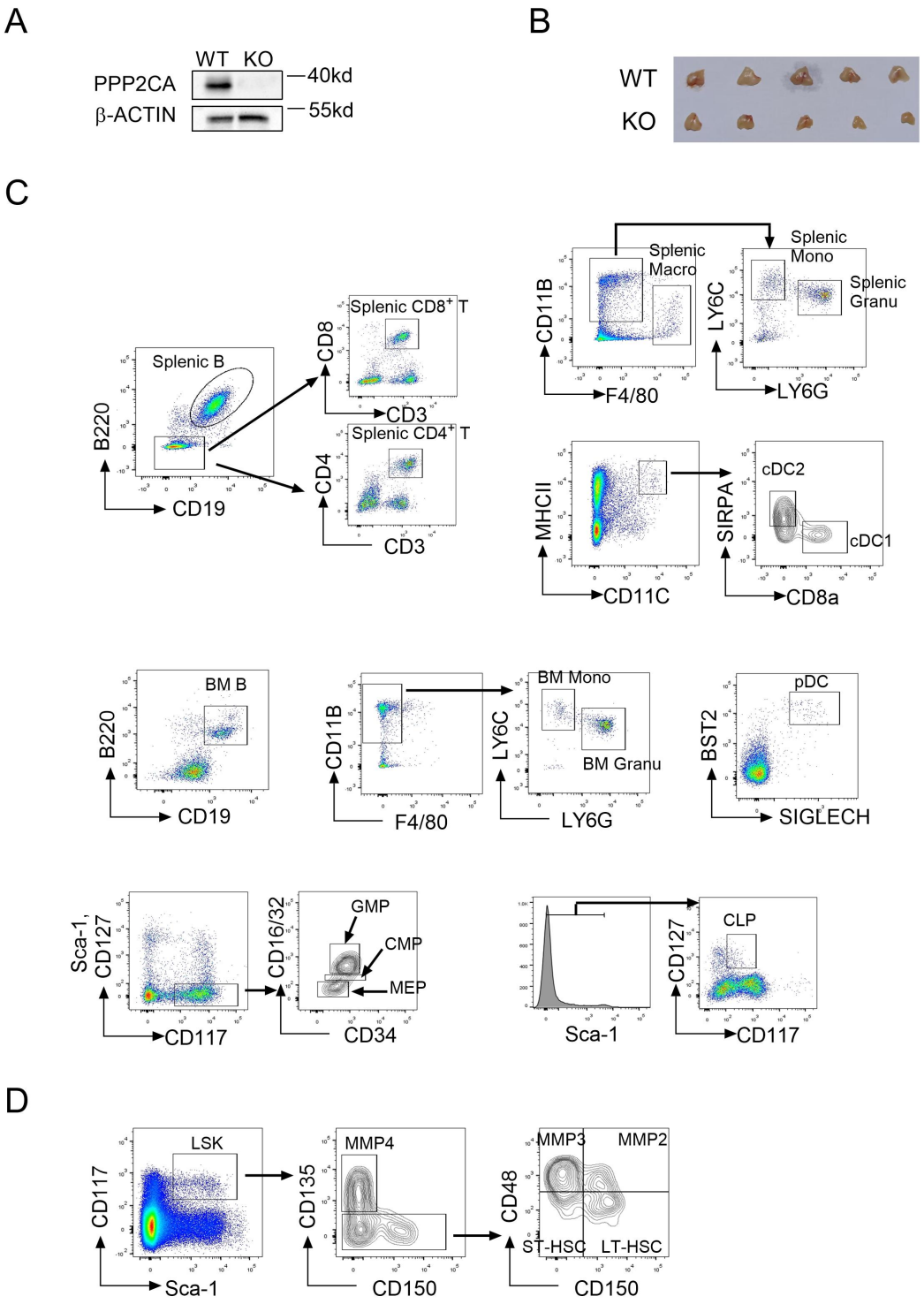

Supplementary Figure 1. The validation of PPP2CA knockout and gating strategies in flow cytometry analysis. (A) Immunoblotting analysis of the KO efficiency of PPP2CA protein in BM Lin$^-$ cells from the tamoxifen pre-treated *Ppp2ca*$^{f/f}$ (WT) and *Ert2*^{cre}*Ppp2ca*$^{f/f}$ (KO) mice. β-ACTIN was used as the internal loading control. Representative data of two repeated experiments. (B) The thymic atrophy observed in *Ppp2ca*-deficient mice. (C) Gating strategies for cell subpopulations. B cells, B220$^+$CD19$^+$; splenic CD4$^+$ T cells, CD19$^-$B220$^-$CD3$^+$CD4$^+$;

splenic $CD8^+$ T cells, $CD19^-B220^-CD3^+CD8^+$; monocytes, $CD11B^+F4/80^-Ly6C^{high}Ly6G^-$; granulocytes, $CD11B^+F4/80^-Ly6C^{low}Ly6G^{high}$; macrophages, $F4/80^+$; pDC, $SIGLECH^+BST2^+$; splenic cDC1, $MHCII^+CD11C^+SIRPA^-CD8\alpha^+$; splenic cDC2, $MHCII^+CD11C^+SIRPA^+CD8\alpha^-$. Lineage cells in BM were removed with lineage cocktail antibodies, and lin^- cells were stained with indicated antibodies. GMP, $Lin^-CD127^-CD117^+Sca\text{-}1^-CD34^+CD16/32^+$; CMP, $Lin^-CD127^-CD117^+Sca\text{-}1^-CD34^+CD16/32^{low/-}$; MEP, $Lin^-CD127^-CD117^+Sca\text{-}1^-CD34^-CD16/32^-$; CLP, $Lin^-CD127^+CD117^{int}Sca\text{-}1^{int}$. (**D**) LSK, $Lin^-CD117^+Scal\text{-}1^+$; LT-HSC, $Lin^-CD117^+Scal\text{-}1^+CD135^-CD150^+CD48^-$; ST-HSC, $Lin^-CD117^+Scal\text{-}1^+CD135^-CD150^-CD48^-$; MPP2, $Lin^-CD117^+Scal\text{-}1^+CD135^-CD150^+CD48^+$; MPP3, $Lin^-CD117^+Scal\text{-}1^+CD135^-CD150^-CD48^+$; MPP4, $Lin^-CD117^+Scal\text{-}1^+CD135^+CD150^-CD48^+$.

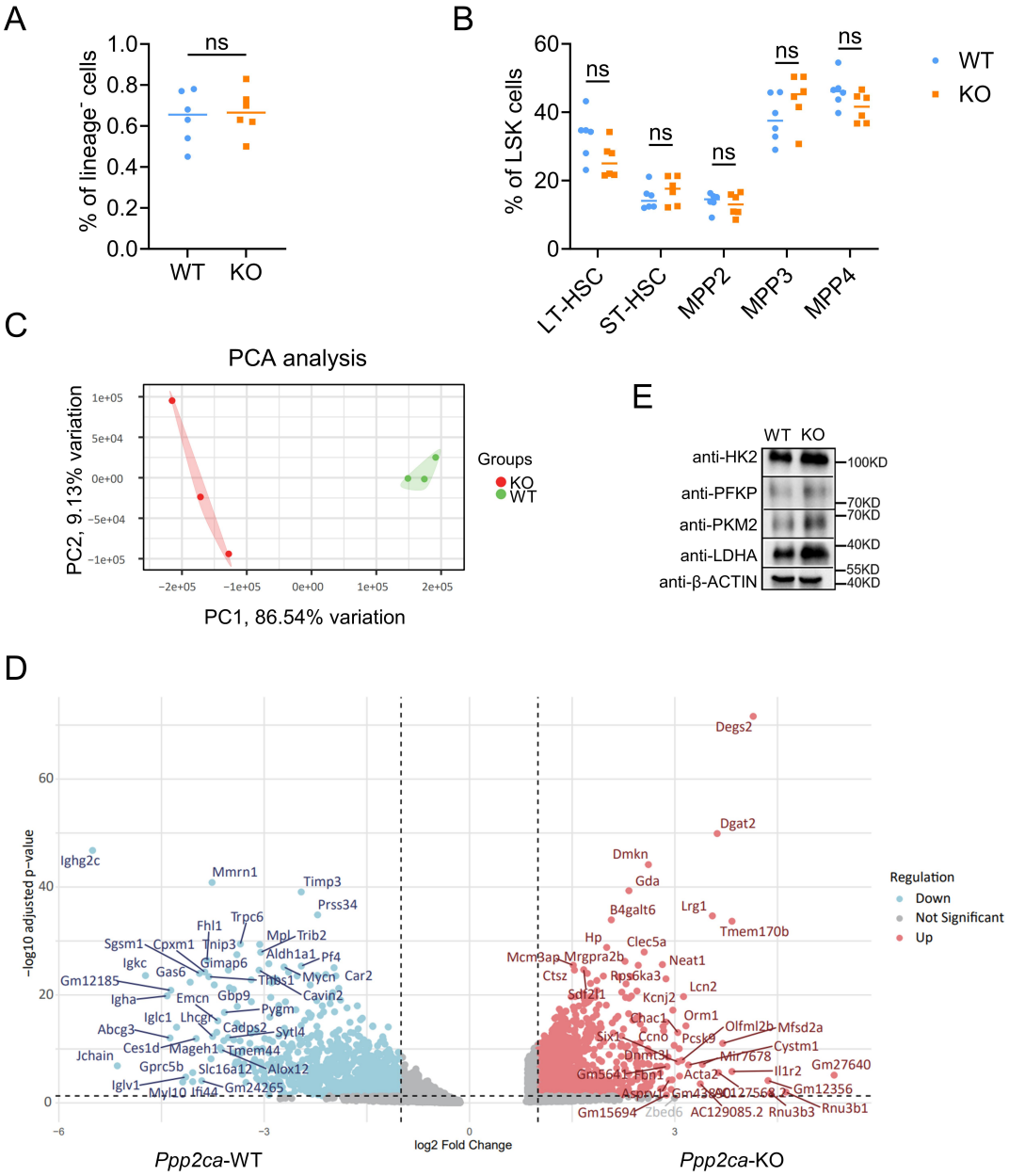

Supplementary Figure 2. (A) The proportion of LSK cells in BM Lin- cells. (B) The proportion of LT-HSC, ST-HSC, MMP2, MMP3 and MMP4 in BM LSK cells. (C) The principal component analysis (PCA) to evaluate global transcriptomic separation between *Ppp2ca*$^{f/f}$ (WT) and *Ert2*^{cre}*Ppp2ca*$^{f/f}$ (KO) LSK cells. (D) A volcano plot was generated to visualize differentially expressed genes (DEGs) between WT and KO LSK cells. The x-axis represents the log2 fold change (log2FC) in gene expression, where positive values indicate upregulation and negative values denote downregulation in KO cells relative to WT cells. The y-axis denotes the -log10 (adjusted p-value [padj]), with higher y-values corresponding to more statistically significant differences in gene expression. (E) WT and KO mice were were treated

with tamoxifen for 5 consecutive days. On day 5 after the last tamoxifen injection, BM LSK cells were isolated from the mice and subjected to immunoblotting analysis to detect the protein levels of HK2, PFKP, PKM2, and LDHA. β-ACTIN was used as the loading control to ensure equal protein loading.

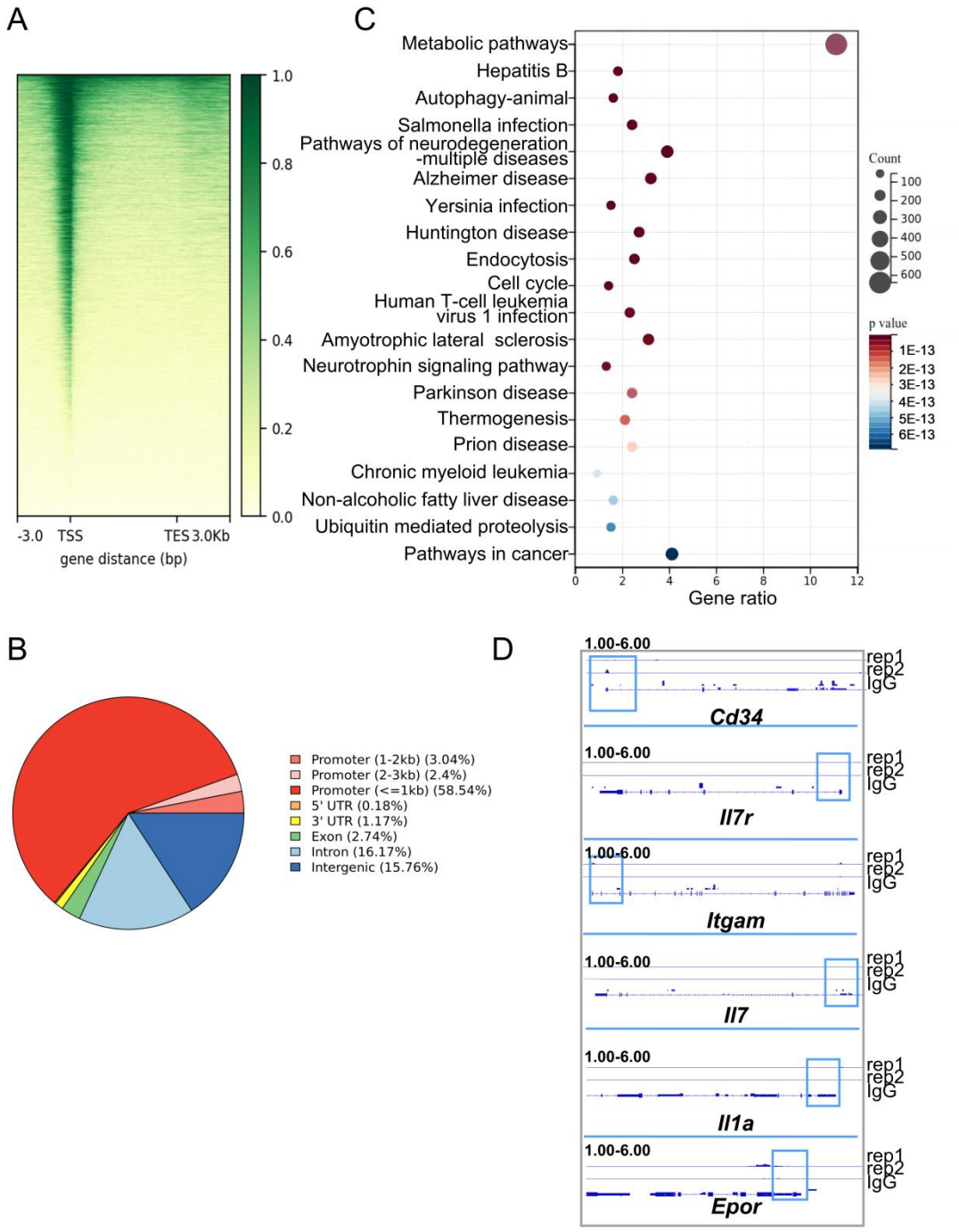

Supplementary Figure 3. *Ppp2ca* keeps the transcription of glycolytic genes in check. (A) Heatmaps depicting the genome-wide occupancy of PPP2CA. Color-scaled intensities depict the genomic occupancy of PPP2CA across all genes, visualized within a 6-kb region extending from 3 kb upstream of the TSS (transcription start site) to 3 kb downstream of the TES (transcription end site). (B) Overview of the genome-wide distribution of PPP2CA binding loci. (C) Enriched pathways of genes with PPP2CA occupancy. (D) The genome browser track depicting PPP2CA signal at representative target genes loci. Blue rectangles highlight the peak regions of PPP2CA enrichment on the promoter target genes. Results from replicate experiments are displayed. rep, repeat.

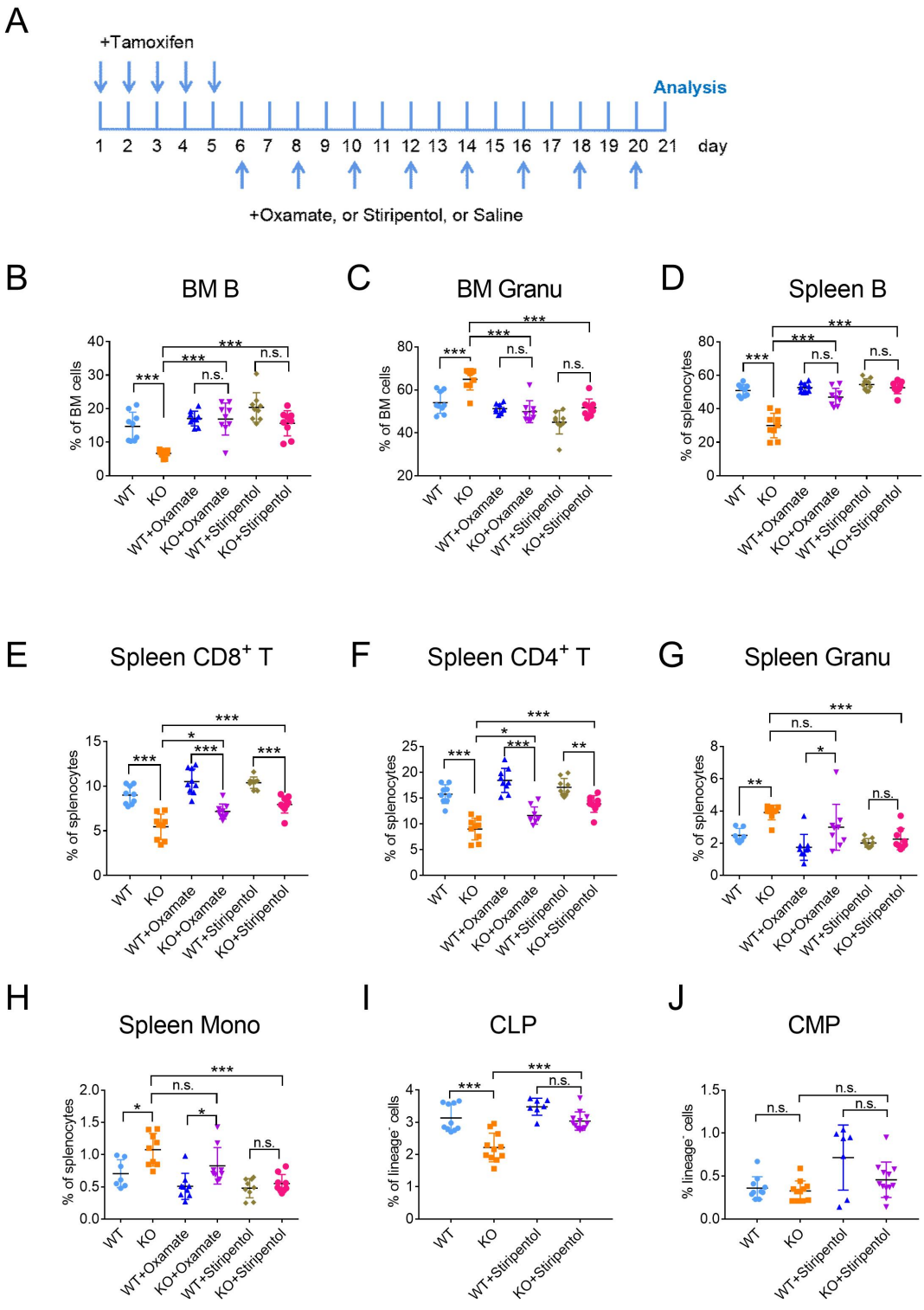

Supplementary Figure 4. Pharmacological interventions targeting lactate metabolism reverse the hematopoietic defects caused by *Ppp2ca* deficiency. (A) Design of the experiments. Tamoxifen pre-treated *Ppp2ca*$^{f/f}$ (WT) and *Ert2*^{cre}*Ppp2ca*$^{f/f}$ (KO) mice were intraperitoneally injected with oxamate, striripentol or saline every other day. (B-J) The proportion of BM B cells (B), BM granulocytes (C), splenic B cells (D), splenic CD8$^+$ T cells (E), splenic CD4$^+$ T cells (F), splenic granulocytes (G),

splenic monocytes (H), BM CLP (I) and BM CMP (J). n=7-12. *p* values were determined by one-way ANOVA. Data are presented as mean ± SEM. (*p<0.05, **p<0.01, ***p<0.001, n.s. not significant).

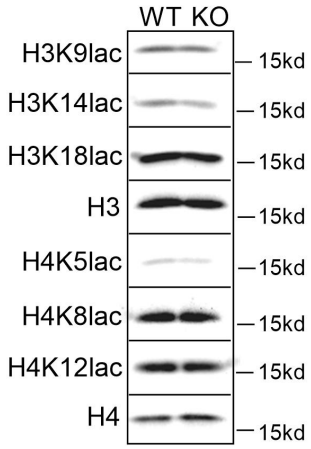

Supplementary Figure 5. Deficiency of *Ppp2ca* exerts no impact on histone lactylation. A screening for differential histone lactylation in Lin$^-$ cells isolated from the BM of tamoxifen treated *Ppp2ca$^{f/f}$* (WT) and *Ert2^{cre}Ppp2ca$^{f/f}$* (KO) mice. The levels of histone lactylation were analyzed by immunoblot.

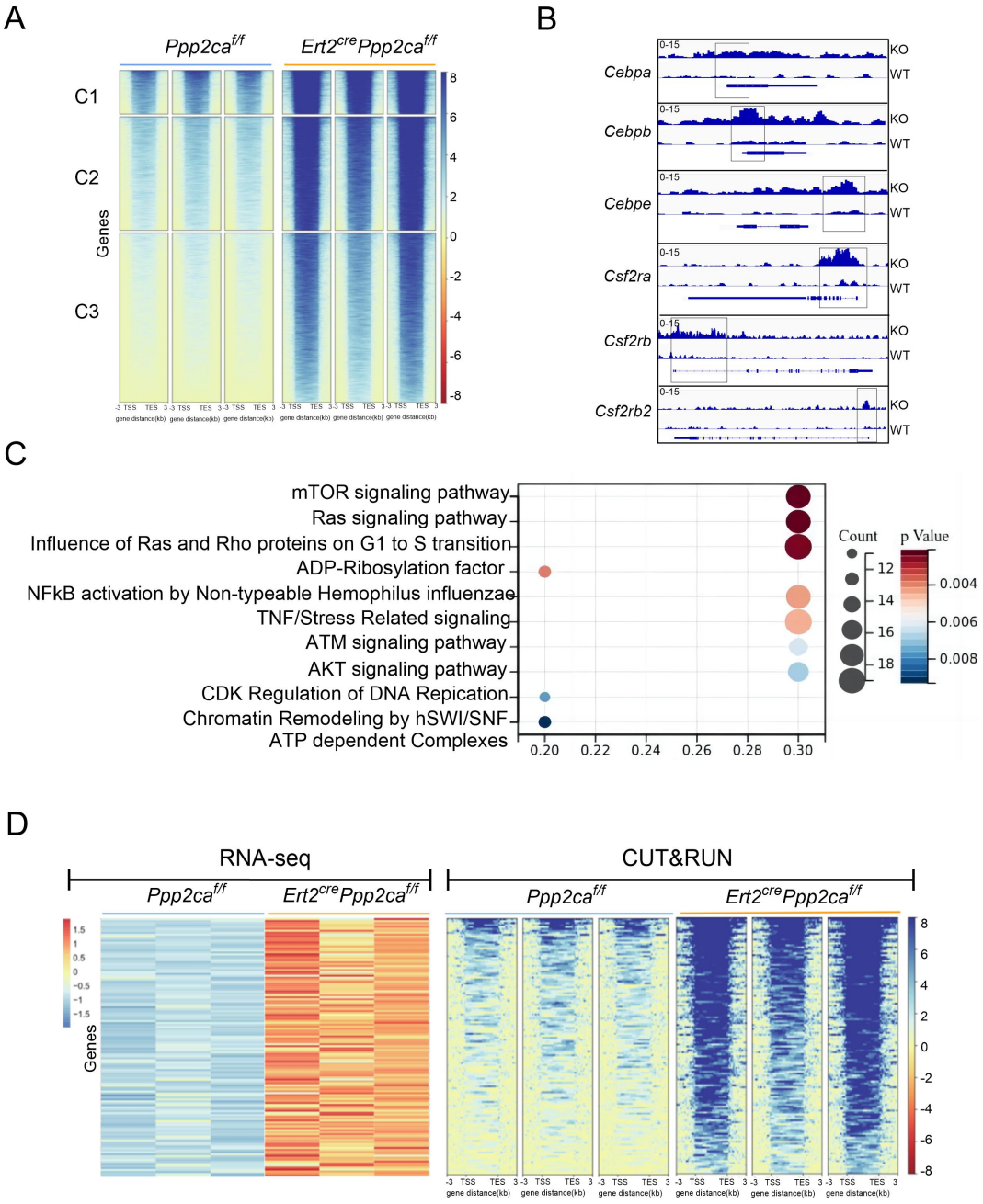

Supplementary Figure 6. *Ppp2ca* deficiency results in elevated acetylation of H3K27. LSK cells were isolated from the BM of tamoxifen treated *Ppp2ca*$^{f/f}$ (WT) and *Ert2*^{cre}*Ppp2ca*$^{f/f}$ (KO) mice. (A) Heatmaps of genome-wide occupancy of H3K27ac in LSK. Color-scaled intensities of all genes at each site within the range of 3kb upstream of the TSS (transcriptional start site) to 3kb downstream of the TES (transcriptional end site) are shown. C1, C2 and C3 indicate gene clusters 1, 2 and 3 with H3K27 acetylation from high to low. (B) The genomic browser track presenting the H3K27ac signal at the loci of representative target genes. The rectangles indicate the peak regions of H3K27ac occupancy on the promoters of target genes. (C) KEGG pathway analysis of genes with elevated H3K27ac modification. (D) Heatmaps depicting the H3K27ac occupancy on genes that were upregulated in the *Ppp2ca*

deficient LSK. The left heatmaps depict the upregulated genes according to the RNA sequencing data in Figure 2, and the right heatmaps illustrate the H3K27ac occupancy on corresponding genes. n=3.

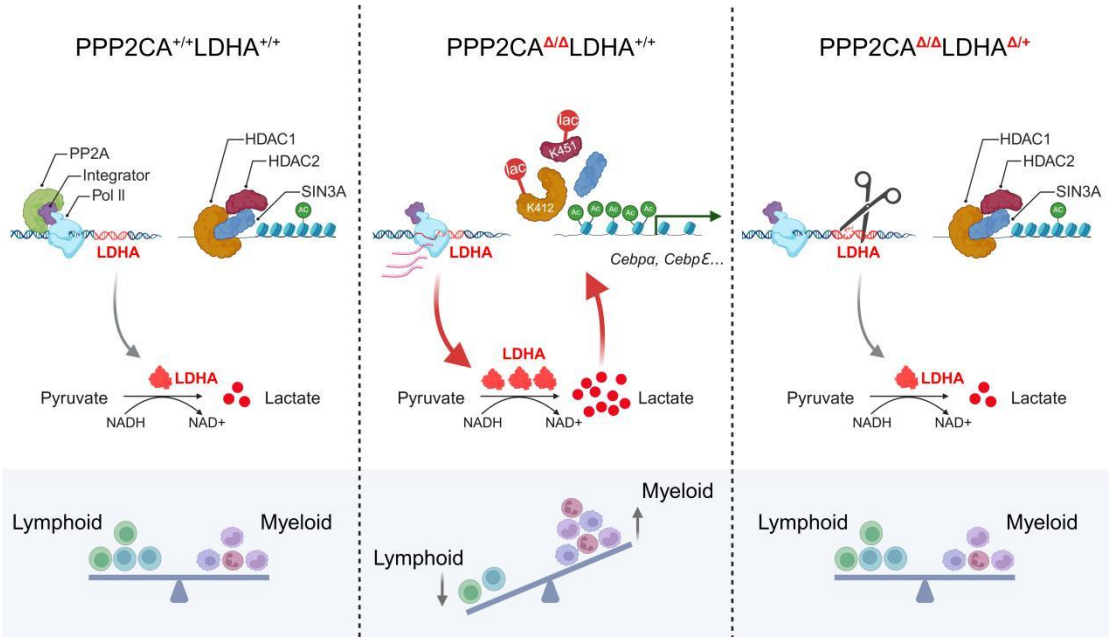

Supplementary Figure 7. Proposed model of this study. *Ppp2ca* deficiency facilitates the RNA Pol II mediated transcriptional initiation of glycolytic genes, including Ldha. Elevated level of lactate leads to lactylation of the 412th lysine (K412) in HDAC1 and the 451st lysine (K451) in HDAC2, impairing the assembly of the HDAC1/2-SIN3A complex on chromatin. Subsequently, the acetylation of histone is enhanced and the expression of myeloid determination genes is upregulated. Consequently, there is an increase in the population of myeloid cells accompanied by a decrease in that of lymphoid cells. Haploid deletion of *Ldha*, the pivotal enzyme responsible for lactate generation, is found to be sufficient to alleviate the myeloid biased differentiation caused by *Ppp2ca* ablation without affecting normal hematopoiesis.

SupplementaryTable 1. List of antibodies and reagents

Antibodies	Source	Cat#
Anti-mouse PDCA1-BV421	BioLegend	127023
Anti-mouse CD4-FITC	BioLegend	100406
Anti-mouse CD34-FITC	BD Bioscience	553733
Anti-mouse B220-PE-CY7	BioLegend	103222
Anti-mouse MHCII-BV510	BioLegend	107636
Anti-mouse CD11c-percpcy5.5	BioLegend	136504
Anti-mouse CD11c-FITC	BioLegend	117306
Anti-mouse CD19-BV510	BioLegend	115546
Anti-mouse Ly-6A/E (Sca-1)-PE-CY7	BioLegend	108114
Anti-mouse CD3-APC	BioLegend	100236
Anti-mouse CD172a-APC	BioLegend	144014
Anti-mouse CD8α-Percp-cy5.5	BioLegend	100736
Anti-mouse SiglecH-PE-CY7	eBioscience	25-0333-82
Anti-mouse CD117-APC	BioLegend	135108
Anti-mouse CD117-PE	BioLegend	135106
Anti-mouse CD127-PE	BioLegend	135010
Anti-mouse CD16/32-APC	BioLegend	101326
Anti-mouse/human CD11b-PE-CY7	BioLegend	101216
Anti-mouse F4/80-PE	BioLegend	123110
Ultra-LEAF™ Purified anti-mouse CD3 Antibody	BioLegend	100238

Ultra-LEAF™ Purified anti-mouse/human CD11b Antibody	BioLegend	101248
Ultra-LEAF™ Purified anti-mouse TER-119 Antibody	BioLegend	116254
Ultra-LEAF ™ Purified anti-mouse/human CD45R/B220 Antibody	BioLegend	103270
Ultra-LEAF™ Purified anti-mouse CD19 Antibody	BioLegend	115570
Ultra-LEAF ™ Purified anti-mouse Ly-6G/Ly-6C (Gr-1) Antibody	BioLegend	108436
Ultra-LEAF™ Purified anti-mouse CD2 Antibody	BioLegend	100119
BioMag Goat anti-Rat IgG (Fc Specific)	Bangs Laboratories	BM548
β-Actin (13E5) Rabbit mAb	Cell Signaling Technology	#4970
Protein G beads	Cell Signaling Technology	#70024
Anti-rabbit IgG, HRP-linked Antibody	Cell Signaling Technology	#7074
Acetyl-Histone H3 (Lys27) (D5E4) XP® Rabbit	Cell Signaling Technology	8173
Histone H3 (D1H2) XP® Rabbit mAb	Cell Signaling Technology	4499
Phospho-Rpb1 CTD (Ser5) (D9N5I) Rabbit mAb	Cell Signaling Technology	13523
PP2A C Subunit Antibody	Cell Signaling	2038

	Technology	
HDAC1 (D5C6U) XP® Rabbit mAb	Cell Signaling Technology	34589
HDAC2 (D6S5P) Rabbit mAb	Cell Signaling Technology	57156
DYKDDDDK Tag (D6W5B) Rabbit mAb	Cell Signaling Technology	14793
PKM2 (D78A4) XP® Rabbit mAb	Cell Signaling Technology	4053
Hexokinase II (C64G5) Rabbit mAb	Cell Signaling Technology	2867
Anti-PFKP 抗体[OTI1D6]	Abcam	ab119796
SIN3A (D1B7) Rabbit mAb	Cell Signaling Technology	7691
Anti-L-Lactyl Lysine Rabbit pAb	PTMBIO	PTM-1401
Lactyl-Histone Antibody Sampler Kit	PTMBIO	PTM-7093
SimpleChIP® Plus Enzymatic Chromatin IP Kit (Magnetic Beads)	Cell Signaling Technology	9005
CellROX™ Green Reagent	ThermoFisher Scientific	C10492
MitoSOX™ Red Reagent	ThermoFisher Scientific	M36008
DCFH-DA	ThermoFisher Scientific	C6827
Red blood cell lysis buffer	ThermoFisher Scientific	00-4333-57

Cell Staining Buffer	BioLegend	420210
Hyperactive Universal CUT&Tag Assay Kit for Illumina	Vazyme	TD903-02
Hyperactive pG-MNase CUT&RUN Assay Kit for Illumina	Vazyme	HD102-01
Pierce™Classic Magnetic IP/Co-IP Kit	ThermoFisher Scientific	88804
SuperBlock™ (TBS) Blocking Buffer	ThermoFisher Scientific	37535
DMEM (Dulbecco's Modified Eagle Medium)	ThermoFisher Scientific	11965092
RPMI 1640 Medium	ThermoFisher Scientific	61870010
Penicillin-Streptomycin	ThermoFisher Scientific	15070063
Fetal Bovine Serum (FBS)	ThermoFisher Scientific	A5670801
BD Horizon™ Fixable Viability Stain 575V	BD Bioscience	565694
L-Lactate Assay Kit (Colorimetric)	Abcam	ab65331
Seahorse XF Glycolytic Rate Assay Kit	Agilent	103344-100
Sodium oxamate	Selleck	S6871
Stiripentol	Selleck	S5266
Tamoxifen	Selleck	S1238
BioMag® Goat anti-Rat IgG	Bangs Labs	BM560
Mouse SCF Recombinant Protein	Peprotech	250-03
Mouse TPO Recombinant Protein	Peprotech	315-14
Mouse FLT3L Recombinant Protein	Peprotech	250-31L
KOD OneTM PCR Master Mix -Blue	TOYOBO	KOD-201
DNase I	Roche	10104159001
Collagenase IV	Sigma-Aldrich	C5138

Supplementary Table 2. Primers used in this study.

Genes	Forward primer (5'-3')	Reverse primer (5'-3')
mouse Ldha	GCCAGCAGTCGCTAGACCTAT	CCAAGTTGTATGACCAGCCCA
mouse Hk2	CTATTTGGCCCCGACTCGC	TGAGCTCCGTGAATAAGCAGG
mouse Pfkp	TTCAGTGCTTGCTGAGTACGG	GCGCTGGAGCTCGAAGAA
mouse Pkm	CTTCAAATCTCCGGGACCCA	GAATGAAGGCAGTCCCTGCT
mouse Atp6v0c	TTCTTCGTTTTTCGGTGTCATGG	TCTAGAGTCCCGCATCGC
mouse Atp5g3	TAAGCCTCTTTTCGCTCCGC	GATCTAGGTGACAGGCGACG
mouse Uqcrfs1	CGAACGAAAGGTCGTCCCTG	GGAAGTGGCCGATAGGACGG
mouse Cd34	CCGGAGCGGTACAGGAGAA	ACTCACGCAGCAGACTCATC
mouse Il7	AGGGCGTGACCCTCTTAATC	CTGAGGAGGCGTCGCTG
mouse Il7r	GCTTAATTCAAGCTGTTTCTGGA	GTTAGAAATGACTCACCATCCTGG
mouse Itgam	GTGCCTGAAATACCACAGTTCAC	CAAGACCCCGCCGACATACC
mouse Cebpa	TTCGATCCGAGACCCGTTTG	CACCCAGTGCCCCAACTG
mouse Cebpb	GCAATGACGCGCACCGA	GGCCGAGCGGGAGGTTTAT
mouse Cebpe	CCTGCCCCTCCCTTAGTCA	CTCCGTCACCAACTCCTACG
mouse Csf2ra	CCCAACCTGCAGATGAGGAA	CTTCCTGCGATGGATGGTGA
mouse Csf2rb	GGGAGGTGGTTATTGCCCTC	CAGCTCTCATGTGCCCTTCA
mouse Csf2rb2	ATGGTGGGGATCGAGCTACT	CAGTGCCCTTTCACAAGCAG